

# HRVGAN: High Resolution Video Generation using Spatio-Temporal GAN

Abhinav Sagar

University of Maryland, College Park, Maryland  
College Park, Maryland

asagar@umd.edu

## Abstract

*High-resolution video generation has emerged as a crucial task in computer vision, with wide-ranging applications in entertainment, simulation, and data augmentation. However, generating temporally coherent and visually realistic videos remains a significant challenge due to the high dimensionality and complex dynamics of video data. In this paper, we propose a novel deep generative network architecture designed specifically for high-resolution video synthesis. Our approach integrates key concepts from Wasserstein Generative Adversarial Networks (WGANs), enforcing a  $k$ -Lipschitz continuity constraint on the discriminator to stabilize training and enhance convergence. We further leverage Conditional GAN (cGAN) techniques by incorporating class labels during both training and inference, enabling class-specific video generation with improved semantic consistency. We provide a detailed layer-wise description of the Generator and Discriminator networks, highlighting architectural design choices promoting temporal coherence and spatial detail. The overall combined architecture, training algorithm, and optimization strategy are thoroughly presented. Our training objective combines a pixel-wise mean squared error loss with an adversarial loss to balance frame-level accuracy and video realism. We validate our approach on benchmark datasets including UCF101, Golf, and Aeroplane, encompassing diverse motion patterns and scene contexts. Quantitative evaluations using Inception Score (IS) and Fréchet Inception Distance (FID) demonstrate that our model significantly outperforms previous state-of-the-art unsupervised video generation methods in terms of both quality and diversity.*

## 1. Introduction

Deep learning approaches to computer vision have traditionally focused on static image analysis, successfully addressing a wide range of tasks such as classification, detection, and segmentation. However, real-world visual data is inherently dynamic, composed of sequences of frames

connected through the temporal dimension. This temporal information carries crucial cues about object motion, scene dynamics, and evolving contexts, enabling richer scene understanding beyond what single images can provide.

Despite this, modeling video data poses unique challenges, primarily due to the increased computational complexity and the need to capture both spatial and temporal dependencies. Static image-based methods are fundamentally limited for tasks such as action recognition and prediction, where understanding motion and temporal progression is essential [13]. Consequently, video-based algorithms capable of modeling temporal dynamics have become a critical area of research.

Generating realistic videos from latent representations is a particularly challenging problem in deep learning. State-of-the-art approaches often suffer from blurriness and lack of temporal coherence, highlighting the difficulty of modeling the complex pixel-wise transformations across frames [30]. Effective video generation requires not only understanding spatial content within each frame but also accurately modeling temporal evolution and uncertainty across frames [29].

To address these challenges, prior works have sought to disentangle spatial and temporal dynamics. Spatial dynamics capture the appearance and structure of objects in individual frames, while temporal dynamics describe their movement and interactions over time. Methods such as 1-D convolutional networks applied over time [21] and recurrent neural networks (RNNs) generating latent codes for frame synthesis [27] have been explored to reduce computational cost while modeling temporal dependencies. However, while 1-D convolutions provide efficiency gains, more expressive 3-D convolutional architectures are necessary for accurately modeling the complex spatiotemporal correlations inherent in high-quality video synthesis.

A notable limitation of many existing video generation models is their narrow focus on specialized tasks or datasets, which hinders their generalizability across different video generation and prediction scenarios. Furthermore, most architectures in the literature are tailored to domain-

specific problems, lacking the flexibility to adapt to broader settings without significant redesign.

In this work, we propose a novel unsupervised generative adversarial network (GAN) architecture designed for high-resolution video generation and prediction. Our approach addresses these limitations by integrating advanced techniques from Wasserstein GANs and conditional GANs, enabling stable training and improved control over generated content. Crucially, our architecture is designed to be generalizable across diverse datasets and tasks, paving the way for more flexible and scalable video generation frameworks.

## 2. Related Work

Generative models have shown significant promise in modeling the complex temporal dynamics inherent in video data. Among these, autoregressive models such as those introduced in [28] sequentially generate frames conditioned on previous ones, capturing temporal dependencies explicitly. Meanwhile, Generative Adversarial Networks (GANs) have gained traction for video generation due to their ability to produce sharp, realistic frames. Notable GAN-based video generation efforts include [33], [1], and [27], each demonstrating varying levels of success in balancing temporal coherence and image fidelity.

The progress of GANs in recent years can largely be attributed to improvements in training stability [22], the introduction of more effective loss functions [7], and advances in architectural design such as progressive growing of GANs [14]. However, despite these advances, applying GANs effectively to video data—especially in the context of action prediction and unsupervised settings—remains relatively underexplored.

A core challenge in GAN training is mode collapse, where the generator produces limited diversity in samples, often generating near-identical outputs. To address this, various strategies have been proposed: multi-generator frameworks that encourage diversity, as in [8], and reconstructor networks that invert generated samples back to latent codes to enforce consistency [24]. Additionally, the progressive growing technique introduced by [14] stabilizes training for high-resolution image synthesis by gradually increasing the network’s capacity and output resolution. Concurrently, improvements in loss formulations such as Wasserstein GAN with Gradient Penalty (WGAN-GP) [2, 10] and perceptual losses [7] have significantly enhanced training dynamics and output quality.

Much of the existing literature on video generation relies on supervised learning paradigms. For example, [30] proposed an unsupervised video generation approach that separates foreground and background by employing two parallel streams in the generator—combining 2D and 3D convolutional layers—and a 3D convolutional discriminator. Sim-

ilarly, [27] introduced a temporal and spatial generator decomposition, but the output resolution was limited to  $64 \times 64$  pixels. Another approach by [21] employed a cascade architecture where a temporal generator composed of 1-D deconvolutional layers transforms a latent vector into a sequence of latent vectors, each fed into an image generator to synthesize frames.

Despite these innovations, most existing methods generate low-resolution videos and are often specialized to particular datasets or problem settings, limiting their general applicability.

In contrast, our work advances the state of the art with the following key contributions:

- We propose a novel GAN architecture for unsupervised high-resolution video generation at  $256 \times 256$  pixels, significantly improving spatial detail and temporal coherence over prior work.
- We provide detailed architectural descriptions of both the generator and discriminator networks, along with comprehensive explanations of our optimization strategies and composite loss functions combining adversarial and pixel-level objectives.
- We rigorously validate our approach on publicly available benchmark datasets—including UCF101, Golf, and Aeroplane—demonstrating strong qualitative and quantitative performance.
- Using standard metrics such as Inception Score (IS) and Fréchet Inception Distance (FID), our network consistently outperforms previous state-of-the-art methods in unsupervised video generation.

## 3. Background

### 3.1. GAN

GANs are a family of unsupervised generative models that learns to generate samples from a given distribution [9]. Given a noise distribution, Generator  $G$  tries to generate samples while the Discriminator  $D$  tries to tell whether the generated samples are from the correct distribution or not. Both the generator and discriminator are trying to fool each other, thus playing a zero-sum game. In other words, both are in a state of Nash Equilibrium. Let  $G$  represent the generator and  $D$  the discriminator, the loss function used for training GAN can be written as shown below:

$$\mathcal{F}(\mathcal{D}, \mathcal{G}) = \mathbb{E}_{\mathbf{x} \sim p_x}[-\log \mathcal{D}(\mathbf{x})] \quad (1)$$

$$+ \mathbb{E}_{\mathbf{z} \sim p_z}[-\log(1 - \mathcal{D}(\mathcal{G}(\mathbf{z})))] \quad (2)$$

where  $z$  is latent vector,  $x$  is data sample,  $p_z$  is probability distribution over latent space and  $p_x$  is probability distribution over data samples. The zero-sum condition is defined as:

$$\min_G \max_D \mathcal{F}(\mathcal{D}, \mathcal{G}) \quad (3)$$

A lot of changes have been proposed over the years to reduce mode collapse and minimize training instability, which are two of the main challenges while training GANs. Some of these changes are using least square loss instead of sigmoid cross entropy loss as shown in [16] and using feature matching and minibatch discrimination as shown in [22].

### 3.2. Wasserstein GAN

A new technique was proposed to minimize the Wasserstein Distance (WD) between the distributions to stabilize training. WD between two distributions was used in [2] is defined in:

$$W(p_r, p_g) = \inf_{\gamma \in \Pi(p_r, p_g)} \mathbb{E}_{(x, y) \sim \gamma} [\|x - y\|] \quad (4)$$

where  $p_r, p_g$  are distributions of real and generated samples and  $\Pi(p_r, p_g)$  is the space of all possible joint probability distributions of  $p_r$  and  $p_g$ .

Another technique, known as weight clipping, was also proposed to enforce the K-Lipschitz constraint. The loss function for training the network is defined as shown in:

$$\mathcal{F}(\mathcal{D}, \mathcal{G}) = \mathbb{E}_{\mathbf{x} \sim p_x} [\mathcal{D}(\mathbf{x})] - \mathbb{E}_{\mathbf{z} \sim p_z} [\mathcal{D}(\mathcal{G}(\mathbf{z}))] \quad (5)$$

$$+ \lambda \mathbb{E}_{\hat{\mathbf{x}} \sim p_x} \left[ (\|\nabla_{\hat{\mathbf{x}}} \mathcal{D}(\hat{\mathbf{x}})\|_2 - 1)^2 \right] \quad (6)$$

Where  $\lambda$  is a regularization parameter.

### 3.3. Conditional GANs

These types of GANs use conditions on the generator to generate samples with desired properties as first shown in [18]. The loss functions for Conditional GANs can be defined as in:

$$\mathcal{F}(\mathcal{D}, \mathcal{G}) = \mathbb{E}_{\mathbf{x} \sim p_x} [-\log \mathcal{D}(\mathbf{x})] + \mathbb{E}_{\mathbf{z} \sim p_z} [-\log(1 - \mathcal{D}(\mathcal{G}(\mathbf{z})))] \quad (7)$$

The conditions could be class labels or the original data sample in the case of video prediction.

## 4. Method

### 4.1. Dataset

The following datasets were used in this work for training and testing our network for video generation:

1. UCF101 Dataset: The purpose of this dataset was to train networks robust for action recognition tasks. It contains 13320 videos of 101 different action categories like Sky Diving, Knitting, and Baseball Pitch [23].

2. Golf and Aeroplane Datasets: It contains  $128 \times 128$  resolution frames, which can be used for evaluating video generative adversarial networks [30] and [15].

### 4.2. Network Architecture

Let input sequence frames of a video be denoted by  $(X = X_1, \dots, X_m)$  and frames to be predicted in sequence by  $(Y = Y_1, \dots, Y_n)$ . Our proposed network for high-resolution video generation operates in two key stages: (1) a novel conditional Generative Adversarial Network (GAN) designed to generate coherent video sequences conditioned on specified action categories, and (2) a reconstruction network equipped with a newly formulated loss function to refine and map generated latent sequences into the pixel space with high fidelity.

In the first stage, the input to the Generator is a sequence of latent noise vectors, each corresponding to a frame in the target video sequence. These latent vectors are conditioned on the action category label, enabling the Generator to produce temporally coherent frame sequences that semantically align with the specified action class. The Generator transforms the input latent sequence into a sequence of synthesized video frames.

The generated video frames are then passed to the Discriminator, which evaluates the authenticity of the sequence by distinguishing between real video samples from the training dataset and the synthetic frames produced by the Generator. This adversarial setup encourages the Generator to produce realistic and temporally consistent videos.

Both Generator and Discriminator networks are trained end-to-end using mini-batch Stochastic Gradient Descent (SGD) with carefully designed loss functions. The Generator loss combines adversarial feedback with a pixel-level reconstruction loss, ensuring both global realism and local detail preservation, while the Discriminator is trained to robustly classify real versus generated frame sequences.

Architecturally, the Generator leverages 3D transposed convolutional (deconvolutional) layers to jointly model spatial and temporal information, allowing for effective synthesis of video frames that capture both appearance and motion. Conversely, the Discriminator employs 3D convolutional layers to analyze the spatiotemporal coherence of input video sequences. To promote stable and efficient training, batch normalization is applied throughout the Generator network, facilitating gradient flow and convergence, whereas instance normalization is utilized in the Discriminator to improve generalization and reduce internal covariate shift.

Regarding activation functions, the Generator uses ReLU nonlinearities to maintain strong gradient signals during training and encourage sparse feature activations, while the Discriminator employs leaky ReLU activations to mitigate the dying ReLU problem and ensure gradient flow even when activations fall below zero.

The network architecture used in this work is shown in Figure 1:

The Generator layer-wise details are shown in Table 1:

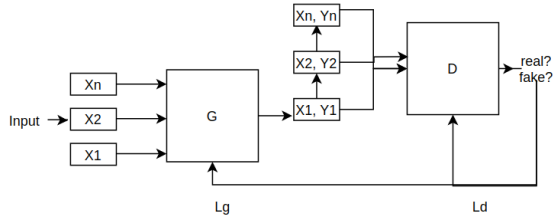


Figure 1. Illustration of the network architecture.

Table 1. Generator architecture layer-wise details.

Generator	Activation	Output shape
Latent vector	-	128×1×1×1
Fully-connected	ReLU	128×1×1×1
DeConv 3×3×3	ReLU	128×4×4×4
Upsample	-	128×8×8×8
DeConv 3×3×3	ReLU	128×8×8×8
DeConv 3×3×3	ReLU	128×8×8×8
Upsample	-	128×8×16×16
DeConv 3×3×3	ReLU	128×8×16×16
DeConv 3×3×3	ReLU	128×8×16×16
Upsample	-	128×8×32×32
DeConv 3×3×3	ReLU	64×8×32×32
DeConv 3×3×3	ReLU	64×8×32×32
Downsample	-	64×16×64×64
Conv 3×3×3	Leaky ReLU	32×16×64×64
Conv 3×3×3	Leaky ReLU	32×16×64×64
Downsample	-	32×16×128×128
Conv 3×3×3	Leaky ReLU	16×16×128×128
Conv 3×3×3	Leaky ReLU	16×16×128×128
Downsample	-	16×32×256×256
Minibatch Stddev	-	129×4×4×4
Conv 3×3×3	Leaky ReLU	8×32×256×256
Fully-connected	linear	1×1×1×128
Fully-connected	linear	1×1×1×1

The Discriminator layer-wise details are shown in Table 2:

### 4.3. Pixel Normalization

To avoid an explosion of parameters in both the generator and the discriminator, feature vectors are normalized at every pixel. We extended the feature vector normalization as proposed by [14] to our spatio-temporal problem.

Let  $a_{x,y,t}$  and  $b_{x,y,t}$  be the original and normalized feature vectors at pixel  $(x, y, t)$  corresponding to spatial and temporal position. The following relation can be written as shown below:

Table 2. Discriminator architecture for generation of 256×256×32 videos

Discriminator	Activation	Output shape
Input Image	-	128×1×1
Conv 1×1×1	Leaky ReLU	128×4×4×4
Conv 3×3×3	Leaky ReLU	128×4×4×4
Conv 3×3×3	Leaky ReLU	128×4×4×4
Downsample	-	128×8×8×8
Conv 3×3×3	Leaky ReLU	128×8×8×8
Conv 3×3×3	Leaky ReLU	128×8×8×8
Downsample	-	128×8×16×16
Conv 3×3×3	Leaky ReLU	128×8×16×16
Conv 3×3×3	Leaky ReLU	128×8×16×16
Downsample	-	128×8×32×32
Conv 3×3×3	Leaky ReLU	64×8×32×32
Conv 3×3×3	LReLU	64×8×32×32
Downsample	-	64×16×64×64
Conv 3×3×3	Leaky ReLU	32×16×64×64
Conv 3×3×3	Leaky ReLU	32×16×64×64
Downsample	-	32×16×128×128
Conv 3×3×3	Leaky ReLU	16×16×128×128
Conv 3×3×3	Leaky ReLU	16×16×128×128
Downsample	-	16×32×256×256
Minibatch Stddev	-	129×4×4×4
Conv 3×3×3	Leaky ReLU	8×32×256×256
Fully-connected	linear	1×1×1×128
Fully-connected	linear	1×1×1×1

$$b_{x,y,t} = \frac{a_{x,y,t}}{\sqrt{\frac{1}{N} \sum_{j=0}^{N-1} (a_{x,y,t}^j)^2 + \epsilon}} \quad (8)$$

where  $\epsilon$  is a constant and  $N$  is number of feature maps used.

### 4.4. Instance Normalization

Instance normalization was used after both 3D convolutional and 3D deconvolutional layers to solve the vanishing gradient problem as defined below:

$$y = \text{ReLU} \left( \sum_{i=0}^d w_i \cdot \text{ReLU} \left( \gamma_i \cdot \frac{x_i - \mu_i}{\sqrt{\sigma_i^2 + \epsilon}} + \beta_i \right) + b \right) \quad (9)$$

Where  $w$  and  $b$  are the weight and bias terms of the 3D convolution layer,  $\gamma$  and  $\beta$  are the weight and bias terms of the Instance Normalization layer,  $\mu$  and  $\sigma$  are the mean and variance of the input.

## 4.5. Loss Functions

Generator in the GAN architecture can be used to predict a sequence of frames  $Y$  from a sequence of frames  $X$  by minimizing the pixel-wise distance between the predicted and the actual frame. The mean square pixel-wise loss function is defined in [Equation 10](#):

$$\mathcal{L}_{mse}(X, Y) = \ell_{mse}(G(X), Y) = \|G(X) - Y\|^2 \quad (10)$$

The binary cross-entropy loss between the actual and predicted frames is defined in [Equation 11](#):

$$L_{bce}(Y, \hat{Y}) = - \sum_i \hat{Y}_i \log(Y_i) + (1 - \hat{Y}_i) \log(1 - Y_i) \quad (11)$$

where both  $Y_i$  and  $\hat{Y}_i$  has values in the range  $[0, 1]$ .

Let  $(X, Y)$  be a sample from the dataset where both  $X$  and  $Y$  denote a sequence of frames as input and to be predicted, respectively. Let  $G$  represent the Generator and  $D$  the Discriminator. The goal is to predict the right frames for both the individual classes represented by 0 and 1. The adversarial loss function used for training the Generator is defined in:

$$\mathcal{L}_{adv}^G(X, Y) = \lambda_1 \sum_{i=1}^N L_{bce}(D_i(X_i, G_i(X_i)) - k, 1) \quad (12)$$

The adversarial loss function used for training the Discriminator is defined in:

$$\mathcal{L}_{adv}^D(X, Y) = \lambda_1 \sum_{i=1}^N L_{bce}(D_i(X_i, Y_i) - k, 1) \quad (13)$$

$$+ \lambda_2 L_{bce}(D_i(X_i, G_i(X)) - k, 0) \quad (14)$$

Where  $\lambda_1, \lambda_2$  are the coefficients to balance the penalty terms.  $\lambda_1, \lambda_2$  are also used to absorb the scale  $k$  caused by the k-Lipschitz constraint on Wasserstein loss.

The mean square loss function and adversarial loss function of the Generator can be combined with equal weights given to both terms, as shown below:

$$\mathcal{L}(X, Y) = \alpha \mathcal{L}_{adv}^G(X, Y) + \beta \mathcal{L}_{mse}(X, Y) \quad (15)$$

Where  $\alpha$  and  $\beta$  are constants with values of 0.5 and 0.5, respectively.

## 4.6. Algorithm

The complete algorithm used in this work is shown below:

---

### Algorithm 1: HRVGAN: High Resolution Video Generation using Spatio-Temporal GAN

---

Initialize learning rates  $\alpha_D$  and  $\alpha_G$ , and weights  $\lambda_{adv}, \lambda_{\ell_{mse}}$

**while** not converged **do**

**Update the Discriminator**  $D$ :

Get  $M$  data samples

$$(X, Y) = (X^{(1)}, Y^{(1)}), \dots, (X^{(M)}, Y^{(M)})$$

$$W_D = W_D - \alpha_D \sum_{i=1}^M \frac{\partial \mathcal{L}_{adv}^D(X^{(i)}, Y^{(i)})}{\partial W_D}$$

**Update the Generator**  $G$ :

Get  $M$  data samples

$$(X, Y) = (X^{(1)}, Y^{(1)}), \dots, (X^{(M)}, Y^{(M)})$$

$$W_G = W_G - \alpha_G \sum_{i=1}^M \left( \lambda_{adv} \frac{\partial \mathcal{L}_{adv}^G(X^{(i)}, Y^{(i)})}{\partial W_G} + \lambda_{\ell_{mse}} \frac{\partial \mathcal{L}_{\ell_{mse}}(X^{(i)}, Y^{(i)})}{\partial W_G} \right)$$

**end**

---

## 4.7. Evaluation Metrics

Various metrics have been proposed for evaluating GANs in the literature. Two of the most common metrics are Inception Score and Fréchet Inception Distance, which are explained below:

1. **Inception Score (IS)** - Inception Score was first proposed in [\[22\]](#) for evaluating GANs. A higher inception score is preferred, which means the model can generate diverse images, thus avoiding the mode collapse issue.

Let  $x$  be samples generated by the generator  $G$ ,  $p(y|x)$  be the distribution of classes for generated samples, and  $p(y)$  be the marginal class distribution. The Inception score is defined as:

$$IS(\mathcal{G}) = \exp(\mathbb{E}_{\mathbf{x} \sim p_g} \mathcal{D}_{KL}(p(y|x) || p(y))) \quad (16)$$

where  $D_{KL}$  is the Kullback-Leibler divergence between  $p(y|x)$  and  $p(y)$ .

2. **Fréchet Inception Distance (FID)** - Another metric to evaluate the quality of generated samples was first proposed by [\[12\]](#).

Let  $D$  represent the CNN used to extract features,  $(m_r, \sigma_r)$  be mean and covariance of features extracted from real samples and  $(m_f, \sigma_f)$  be mean and covariance of features

extracted from fake samples with  $D$ , then the Fréchet Inception distance is defined as:

$$d^2((m_r, \Sigma_r), (m_f, \Sigma_f)) = \|m_r - m_f\|_2^2 \quad (17)$$

$$+ \text{Tr} \left( \Sigma_r + \Sigma_f - 2 (\Sigma_r \Sigma_f)^{\frac{1}{2}} \right) \quad (18)$$

Fréchet Inception Distance is more accurate than Inception Score as it compares summary statistics of generated samples and real samples. A lower FID is preferred for better-performing generative models.

## 5. Results and Discussion

The Inception Scores of our proposed model compared to existing approaches on the UCF101 dataset are summarized in [Table 3](#). Our method achieves a significant improvement over prior state-of-the-art models, indicating superior generative quality and diversity in the synthesized videos.

Table 3. Comparison of Inception Scores on the UCF101 dataset. Higher scores indicate better video quality and diversity.

Model	Inception Score
VGAN [30]	8.18
TGAN [21]	11.85
MoCoGAN [27]	12.42
Ours	<b>14.29</b>

We further evaluate our network’s performance using the Fréchet Inception Distance (FID) metric on the Golf and Aeroplane datasets, as shown in [Table 4](#). The FID score measures the similarity between the distributions of real and generated videos, with lower values indicating better generation quality. Our model consistently outperforms both VGAN and TGAN by achieving substantially lower FID scores across both datasets.

Table 4. Quantitative comparison of FID scores on Golf and Aeroplane datasets. Lower FID scores indicate better video generation quality.

Model	FID Score (Golf)	FID Score (Aeroplane)
VGAN [30]	113,007	149,094
TGAN [21]	112,029	120,417
Ours	<b>102,584</b>	<b>104,036</b>

To demonstrate the smoothness and semantic consistency of our learned latent space, we perform linear interpolation experiments. [Figure 2](#) illustrates the linear interpolation results on the Golf dataset, where gradual transitions



Figure 2. Linear interpolation in latent space generating samples from the Golf dataset, showing smooth transitions between video frames.

between video samples highlight the model’s ability to capture meaningful latent representations.

Similarly, [Figure 3](#) presents latent space interpolation on the Aeroplane dataset, further confirming the model’s capacity for generating coherent intermediate video frames across distinct samples.

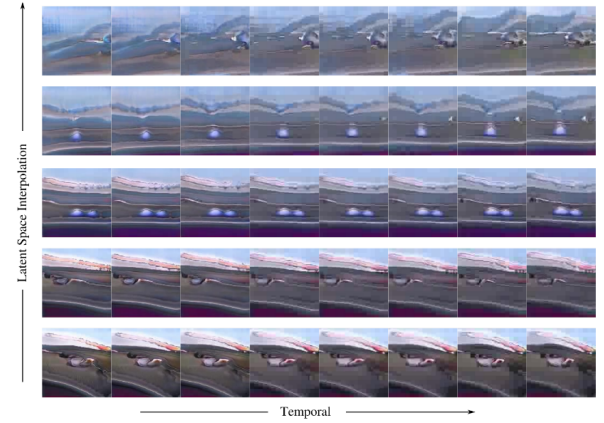


Figure 3. Latent space interpolation results on the Aeroplane dataset, illustrating smooth generation between video samples.

Finally, qualitative results on the UCF101 dataset are shown in [Figure 4](#). Here, we present generated video frames for two action classes: JumpingJack (top row) and TaiChi (bottom row), each consisting of 8 consecutive frames synthesized from random noise. The results demonstrate the temporal coherence and high visual fidelity of our generated videos.



Figure 4. Generated frames on UCF101 dataset for JumpingJack (1st row) and TaiChi (2nd row) actions. Each sequence shows 8 frames generated from random latent vectors, highlighting temporal consistency and realism.

## 6. Conclusions

In this paper, we propose a novel neural network architecture leveraging generative models for unsupervised video generation. Our approach extends the original GAN framework and is trained using mini-batch stochastic gradient descent. The training objective combines a mean squared pixel loss with an adversarial loss constrained by a  $k$ -Lipschitz condition, inspired by Wasserstein GANs. We provide comprehensive details on the network architecture, optimization strategy, and the full algorithmic pipeline. Experimental results on the UCF101, Golf, and Aeroplane datasets demonstrate that our model surpasses existing state-of-the-art methods, evaluated through Inception Score and Fréchet Inception Distance metrics. Additionally, we showcase smooth linear interpolations in the latent space for the Golf and Aeroplane datasets, along with qualitative frame generation results on UCF101.

## References

[1] Dinesh Acharya, Zhiwu Huang, Danda Pani Paudel, and Luc Van Gool. Towards high resolution video generation with progressive growing of sliced wasserstein gans. *arXiv preprint arXiv:1810.02419*, 2018. 2

[2] Martin Arjovsky, Soumith Chintala, and Léon Bottou. Wasserstein gan. *arXiv preprint arXiv:1701.07875*, 2017. 2, 3

[3] Haoye Cai, Chunyan Bai, Yu-Wing Tai, and Chi-Keung Tang. Deep video generation, prediction and completion of human action sequences. In *Proceedings of the European Conference on Computer Vision (ECCV)*, pages 366–382, 2018.

[4] Joao Carreira and Andrew Zisserman. Quo vadis, action recognition? a new model and the kinetics dataset. In *proceedings of the IEEE Conference on Computer Vision and Pattern Recognition*, pages 6299–6308, 2017.

[5] Aidan Clark, Jeff Donahue, and Karen Simonyan. Efficient video generation on complex datasets. *arXiv preprint arXiv:1907.06571*, 2019.

[6] Emily Denton and Rob Fergus. Stochastic video generation with a learned prior. *arXiv preprint arXiv:1802.07687*, 2018.

[7] Ishan Deshpande, Ziyu Zhang, and Alexander G Schwing. Generative modeling using the sliced wasserstein distance. In *Proceedings of the IEEE conference on computer vision and pattern recognition*, pages 3483–3491, 2018. 2

[8] Arnab Ghosh, Viveka Kulharia, Vinay P Namboodiri, Philip HS Torr, and Puneet K Dokania. Multi-agent diverse generative adversarial networks. In *Proceedings of the IEEE conference on computer vision and pattern recognition*, pages 8513–8521, 2018. 2

[9] Ian Goodfellow, Jean Pouget-Abadie, Mehdi Mirza, Bing Xu, David Warde-Farley, Sherjil Ozair, Aaron Courville, and Yoshua Bengio. Generative adversarial nets. In *Advances in neural information processing systems*, pages 2672–2680, 2014. 2

[10] Ishaan Gulrajani, Faruk Ahmed, Martin Arjovsky, Vincent Dumoulin, and Aaron C Courville. Improved training of wasserstein gans. In *Advances in neural information processing systems*, pages 5767–5777, 2017. 2

[11] Jiawei He, Andreas Lehrmann, Joseph Marino, Greg Mori, and Leonid Sigal. Probabilistic video generation using holistic attribute control. In *Proceedings of the European Conference on Computer Vision (ECCV)*, pages 452–467, 2018.

[12] Martin Heusel, Hubert Ramsauer, Thomas Unterthiner, Bernhard Nessler, and Sepp Hochreiter. Gans trained by a two time-scale update rule converge to a local nash equilibrium. In *Advances in neural information processing systems*, pages 6626–6637, 2017. 5

[13] De-An Huang, Vignesh Ramanathan, Dhruv Mahajan, Lorenzo Torresani, Manohar Paluri, Li Fei-Fei, and Juan Carlos Niebles. What makes a video a video: Analyzing temporal information in video understanding models and datasets. In *Proceedings of the IEEE Conference on Computer Vision and Pattern Recognition*, pages 7366–7375, 2018. 1

[14] Tero Karras, Timo Aila, Samuli Laine, and Jaakko Lehtinen. Progressive growing of gans for improved quality, stability, and variation. *arXiv preprint arXiv:1710.10196*, 2017. 2, 4

[15] Bernhard Kratzwald, Zhiwu Huang, Danda Pani Paudel, and Luc Van Gool. Towards an understanding of our world by ganing videos in the wild. *CoRR, abs/1711.11453*, 2017. 3

[16] Xudong Mao, Qing Li, Haoran Xie, Raymond YK Lau, Zhen Wang, and Stephen Paul Smolley. Least squares generative adversarial networks. In *Proceedings of the IEEE international conference on computer vision*, pages 2794–2802, 2017. 3

[17] Luke Metz, Ben Poole, David Pfau, and Jascha Sohl-Dickstein. Unrolled generative adversarial networks. *arXiv preprint arXiv:1611.02163*, 2016.

[18] Mehdi Mirza and Simon Osindero. Conditional generative adversarial nets. *arXiv preprint arXiv:1411.1784*, 2014. 3

[19] Junting Pan, Chengyu Wang, Xu Jia, Jing Shao, Lu Sheng, Junjie Yan, and Xiaogang Wang. Video generation from single semantic label map. In *Proceedings of the IEEE Conference on Computer Vision and Pattern Recognition*, pages 3733–3742, 2019.

[20] Masaki Saito and Shunta Saito. Tganv2: Efficient training of large models for video generation with multiple subsampling layers. *arXiv preprint arXiv:1811.09245*, 2018.

[21] Masaki Saito, Eiichi Matsumoto, and Shunta Saito. Temporal generative adversarial nets with singular value clipping.

In *Proceedings of the IEEE international conference on computer vision*, pages 2830–2839, 2017. [1](#), [2](#), [6](#)

[22] Tim Salimans, Ian Goodfellow, Wojciech Zaremba, Vicki Cheung, Alec Radford, and Xi Chen. Improved techniques for training gans. In *Advances in neural information processing systems*, pages 2234–2242, 2016. [2](#), [3](#), [5](#)

[23] Khurram Soomro, Amir Roshan Zamir, and Mubarak Shah. Ucf101: A dataset of 101 human actions classes from videos in the wild. *arXiv preprint arXiv:1212.0402*, 2012. [3](#)

[24] Akash Srivastava, Lazar Valkov, Chris Russell, Michael U Gutmann, and Charles Sutton. Veegan: Reducing mode collapse in gans using implicit variational learning. In *Advances in Neural Information Processing Systems*, pages 3308–3318, 2017. [2](#)

[25] Ximeng Sun, Huijuan Xu, and Kate Saenko. A two-stream variational adversarial network for video generation. *arXiv preprint arXiv:1812.01037*, 2018.

[26] Ruben Rodriguez Torrado, Ahmed Khalifa, Michael Cerny Green, Niels Justesen, Sebastian Risi, and Julian Togelius. Bootstrapping conditional gans for video game level generation. *arXiv preprint arXiv:1910.01603*, 2019.

[27] Sergey Tulyakov, Ming-Yu Liu, Xiaodong Yang, and Jan Kautz. Mocogan: Decomposing motion and content for video generation. In *Proceedings of the IEEE conference on computer vision and pattern recognition*, pages 1526–1535, 2018. [1](#), [2](#), [6](#)

[28] Aaron Van den Oord, Nal Kalchbrenner, Lasse Espeholt, Oriol Vinyals, Alex Graves, et al. Conditional image generation with pixelcnn decoders. In *Advances in neural information processing systems*, pages 4790–4798, 2016. [2](#)

[29] Ruben Villegas, Jimei Yang, Yuliang Zou, Sungryull Sohn, Xunyu Lin, and Honglak Lee. Learning to generate long-term future via hierarchical prediction. *arXiv preprint arXiv:1704.05831*, 2017. [1](#)

[30] Carl Vondrick, Hamed Pirsiavash, and Antonio Torralba. Generating videos with scene dynamics. In *Advances in neural information processing systems*, pages 613–621, 2016. [1](#), [2](#), [3](#), [6](#)

[31] Chaoyue Wang, Chang Xu, Chaohui Wang, and Dacheng Tao. Perceptual adversarial networks for image-to-image transformation. *IEEE Transactions on Image Processing*, 27(8):4066–4079, 2018.

[32] Yaohui Wang, Piotr Bilinski, Francois Bremond, and Antitza Dantcheva. Imaginator: Conditional spatio-temporal gan for video generation. In *The IEEE Winter Conference on Applications of Computer Vision*, pages 1160–1169, 2020.

[33] Wei Xiong, Wenhan Luo, Lin Ma, Wei Liu, and Jiebo Luo. Learning to generate time-lapse videos using multi-stage dynamic generative adversarial networks. In *Proceedings of the IEEE Conference on Computer Vision and Pattern Recognition*, pages 2364–2373, 2018. [2](#)

[34] Ceyuan Yang, Zhe Wang, Xinge Zhu, Chen Huang, Jianping Shi, and Dahua Lin. Pose guided human video generation. In *Proceedings of the European Conference on Computer Vision (ECCV)*, pages 201–216, 2018.